

Chalmers Publication Library



This paper is the final draft of a paper submitted to and accepted for publication in *International Journal of Geomechanics*

The final version of the record is available
at: [http://dx.doi.org/10.1061/\(ASCE\)GM.1943-5622.0000267](http://dx.doi.org/10.1061/(ASCE)GM.1943-5622.0000267)

(Article begins on next page)

Comparison of Anisotropic Rate-Dependent Models for Modelling Consolidation of Soft Clays

M. Karstunen¹; M. Rezaia²; N. Sivasithamparam³; and Z.-Y. Yin⁴

Abstract: Two recently proposed anisotropic rate-dependent models are used to simulate the consolidation behaviour of two soft natural clays: Murro clay and Haarajoki clay. The rate-dependent constitutive models include the EVP-SCLAY1 model and the Anisotropic Creep Model (ACM). The two models are identical in the way the initial anisotropy and the evolution of anisotropy are simulated, but differ in the way the rate-effects are taken into consideration. The models are compared first at the element level against laboratory data and then at boundary value level against measured field data from instrumented embankments on Murro and Haarajoki clays. The numerical simulations suggest that at element the EVP-SCLAY1 model is able to give a better representation of the clay response under oedometric loading than ACM, when the input parameters are defined objectively. However, at boundary value level the issue is not as straightforward, and the appropriateness of the constitutive model may depend heavily on the in situ overconsolidation ratio (OCR).

¹ Professor, Dept. of Civil and Environmental Engineering, Chalmers Univ. of Technology, SE 412 96 Gothenburg, Sweden, and Dept. of Civil and Environmental Engineering, Univ. of Strathclyde, John Anderson Building, 107 Rottenrow, Glasgow G4 0NG, UK; and Docent at Aalto Univ., School of Science and Technology, Finland. E-mail: minna.karstunen@chalmers.se.

² Lecturer, School of Civil Engineering and Surveying, Univ. of Portsmouth, Portland Building, Portland Street, Portsmouth PO1 3AH, UK; formerly at Dept. of Civil and Environmental Engineering, Univ. of Strathclyde, John Anderson Building, 107 Rottenrow, Glasgow G4 0NG, UK. E-mail: mohammad.rezaia@port.ac.uk.

³ Marie Curie Post-Doctoral Fellow, Dept. of Civil and Environmental Engineering, Univ. of Strathclyde, John Anderson Building, 107 Rottenrow, Glasgow G4 0NG, UK, and Plaxis bv, Delft, 2628 XJ, The Netherlands. E-mail: ns@plaxis.com.

⁴ Professor, Center for Marine Geotechnics Research, Dept. of Civil Engineering, Shanghai Jiao Tong Univ., Shanghai 200240, PR China. E-mail: zhenyu.yin@gmail.com.

Introduction

Creep and rate-dependence have fascinated geotechnical engineers since early 1920's, but it is only relatively recently that comprehensive rate-dependent constitutive models try to account some fundamental features of natural soil behaviour, such as anisotropy and/or the effect of apparent bonding (see e.g. Zhou et al. 2006; Leoni et al. 2008; Hinchberger and Qu 2009; Karstunen and Yin 2010; Yin et al. 2011). The aim of this paper is to compare objectively the predictions by two anisotropic rate-dependent models: the EVP-SCLAY1 model (Karstunen and Yin 2010) which is an overstress model (Perzyna 1963) and the Anisotropic Creep model (ACM) proposed by Leoni et al. (2008). First, the models are compared at element level against laboratory data. Following that, the comparisons are extended to boundary value level, considering two instrumented embankments on soft clay, namely Murro test embankment (Koskinen et al. 2002) and Haarajoki embankment (FinnRA 1997) in Finland. For the sake of simplicity, the effects of apparent bonding and destructuration of the rate-dependent behaviour are ignored; although, as demonstrated by several researchers e.g. Hinchberger and Qu (2009) and Yin et al. (2010), this is necessary for modelling certain phenomena, such as strain softening, tertiary creep and creep rupture.

ACM and EVP-SCLAY1 Models

The two models, ACM and EVP-SCLAY1, are identical in the way the initial anisotropy and the evolution of anisotropy are modelled, but differ in the way the rate-effects are accounted for. The complete formulations can be found in Appendix A. The initial anisotropy is modelled by defining anisotropic surfaces, attributed to the past history of the soil deposit, which define the boundary between large irrecoverable strains and relatively small strains. These surfaces in stress space are analogous to the anisotropic yield surface in the rate-

independent S-CLAY1 model (Wheeler et al. 2003). Similarly to the S-CLAY1 model, it is assumed that due to subsequent loading that produces irrecoverable strains, there is an evolution in the orientations of these surfaces as a function of irrecoverable volumetric and shear strain increments. As demonstrated by Karstunen and Koskinen (2008), this offers a simple way to represent extremely well the evolution of anisotropy for reconstituted clays. When combined with a destructuration law, it can be extended to account for the large strain behaviour of natural clays (Karstunen and Koskinen 2004; Karstunen et al. 2005).

In the case of the EVP-SCLAY1 model (Karstunen and Yin 2010), this boundary surface is called a static yield surface [see Fig. 1 (a)], and it is assumed that no rate-dependent behaviour occurs when the stresses are within the surface. This basically means that there is a threshold value of effective stresses which needs to be exceeded before rate-dependent behaviour starts, as discussed by Qu et al. (2010). In contrast, in the ACM model, the boundary between the large irrecoverable strains and the relatively small strains is called normal consolidation surface (NCS) [see Fig. 1 (b)] and it is assumed that creep strains occur even in the overconsolidated range, i.e. when the current stress surface in Fig. 1(b) is smaller than the NCS.

The incremental viscoplastic strains in the EVP-SCLAY1 model (Karstunen and Yin 2010) can be calculated as

$$\dot{\varepsilon}_{ij}^{vp} = \mu \left\langle \exp \left[N \cdot \left(\frac{p_m'^d}{p_m'^s} - 1 \right) \right] - 1 \right\rangle \frac{\partial f_d}{\partial \sigma'_{ij}} \quad (1)$$

where μ is referred to as the fluidity parameter; $\langle \rangle$ are McCauley brackets; N is the strain-rate coefficient relating to the strain-rate effect on shear strength and preconsolidation pressure. N and μ are therefore the key parameters controlling the viscoplastic strain-rate. Symbols $p_m'^d$ and $p_m'^s$ represent the size of the dynamic loading surface and the static yield

surface, respectively [see Fig. 1(a)] and f_d is the viscoplastic potential function, represented by the dynamic loading surface.

In ACM, the incremental volumetric creep strains are calculated as

$$\dot{\varepsilon}_{vol}^c = \frac{\mu^*}{\tau} \left(\frac{1}{p'_p / p'_{eq}} \right)^\beta \quad (2)$$

where $\beta = (\lambda^* - \kappa^*) / \mu^*$ is the creep exponent, with λ^* , κ^* and μ^* being the modified compression, swelling and creep indexes; τ is a reference time (equal to 1 day for conventional oedometer test) and p'_p and p'_{eq} refer to the sizes of the normal consolidation surface and the current stress surface [see Fig.1(b)]. Therefore, by comparing Eqs. (1) and (2), it becomes clear that with ACM creep strains will be predicted even at overconsolidated range, in contrast to EVP-SCLAY1, whilst both models relate the actual creep rate somehow to the relative sizes of the respective surfaces shown in Fig. 1.

The advantage of ACM over EVP-SCLAY1 is that it is possible to derive the required soil constants for ACM directly from the experimental tests, whilst the viscosity coefficients of the EVP-SCLAY1 require calibration, as shown by Karstunen and Yin (2010). Both models have been implemented in the Plaxis 2D and 3D finite element code as user-defined soil models, hence enabling the use of the models both at element level and boundary value level.

Determination of Model Parameters

The EVP-SCLAY1 and ACM models involve a number of soil constants and state variables that can be classified in three groups, as follows:

- Parameters which are similar to the Modified Cam Clay parameters include soils constants ν' (Poisson's ratio), M (stress ratio at critical state), λ (slope of the normal

compression line) and κ (slope of the swelling/recompression line). In ACM the modified compression and swelling indexes, where $\lambda^* = \lambda/(1+e)$ and $\kappa^* = \kappa/(1+e)$, are used. Furthermore, the initial values for two state variables, namely e_0 (initial void ratio) and p_{m0} (initial size of the yield surface) are required. In the context of finite element analyses, the initial value of p_{m0} is calculated based on the OCR (vertical overconsolidation ratio) or POP (pre-overburden pressure), normally consolidated K_0^{NC} value (lateral earth pressure at rest, estimated by Jaky's formula) and the initial vertical effective stress.

- Parameters describing initial anisotropy and its evolution include soil constants ω (rate of rotation of the surfaces) and ω_d (relative rate of surface rotation). The latter can be theoretically derived based on M values (see Wheeler et al. 2003 for details). Furthermore, the initial values of the fabric tensor describing the anisotropy of the fabric (i.e. the arrangement of particles and particle contacts) need to be defined. For deposits which have experienced 1D consolidation under their self-weight without significant erosion or unloading, it can be assumed that the fabric is initially cross-anisotropic. In this special case, the components of the fabric tensor can be calculated using a scalar value α_0 , which similarly to ω_d is theoretically simply a function of M (see Wheeler et al. 2003 for details).
- Parameters describing viscosity require the input of two viscosity coefficients. These are soil constants N (strain rate coefficient) and μ (fluidity coefficient) for EVP-SCLAY1 (see Karstunen and Yin 2010 for details), and μ^* (modified creep index) and τ (reference time, which is linked to the definition of vertical preconsolidation stress) for ACM (see Leoni et al. 2008 for details).

Although these models have a relatively large number of parameters, most of them have a clear physical meaning, and hence they can be determined in a relatively straightforward manner (Karstunen and Yin 2010).

Model Parameters for Murro and Haarajoki Clays

Murro clay (Koskinen et al. 2002) is a 23 m thick sulphide-rich silty clay deposit located near the town of Seinäjoki in Finland that has been a subject of many studies (see e.g. Koskinen et al. 2002; Karstunen and Koskinen 2004; Karstunen et al. 2005; Karstunen and Yin 2010) due to a well-instrumented test embankment, built in 1993, and extensive programmes of specialist laboratory testing. The deposit can be roughly divided into two main layers: a 1.6 m thick overconsolidated dry crust and an underlying thick layer of almost normally consolidated soft clay. The most compressible layers are at depths between 1.6 and 7 m, which is the focus of the element-level tests presented in this paper. Murro clay is highly anisotropic with regards of yielding, as demonstrated by the yield points in the $p' - q$ plane in Fig. 2. Murro clay is moderately sensitive, with sensitivity around 6-14.

Haarajoki in the Southern Finland is the location of an instrumented embankment forming a noise barrier, which was the subject of an international competition organized by the Finnish National Road Administration (FinnRA 1997). Half of the 100m long embankment has been constructed on the natural clay, whilst the rest of the embankment is on vertical drains. In contrast to Murro clay, Haarajoki clay is lightly overconsolidated, with an estimated vertical pre-overburden pressure >30 kPa. The deposit can be characterized by a high degree of anisotropy and some apparent interparticle bonding, with sensitivity varying from almost zero at the surface to over 50 at a depth of 15 m (Yildiz et al. 2009b).

Conventional oedometer test results, combined with the results from drained and/or undrained triaxial tests on Murro and Haarajoki clays have been used for determination of

average parameter values for the EVP-SCLAY1 and ACM models. As there is natural variation between clay samples further magnified by potential sample disturbance, for each clay layer a number of tests of the same type were used to estimate the average values of parameters. A number of publications are available which report the required parameter values (e.g. Karstunen et al. 2005; Yildiz et al. 2009b; Karstunen and Yin 2010). However, the procedure for calibrating model parameters is presented briefly as follows:

- λ and κ are measured from conventional 1-day loading oedometer tests on intact samples (from which the corresponding λ^* and κ^* values for ACM model can be calculated). For natural clays, λ and λ^* are not soil constants, and usually the highest values derived from oedometer tests should be used. M is derived from either drained or consolidated undrained triaxial compression test results. The value for Poisson's ratio for each clay is selected according to previous experience (e.g. Karstunen et al. 2005; Karstunen and Yin 2010; Yin et al. 2011), as the triaxial shear tests did not involve such unloading reloading stages that would enable direct determination of purely elastic ν' values.
- The anisotropy parameters α_{K0} and ω_d can be calculated from M values, and the values for ω can be obtained either by simulating specialist triaxial tests (see Wheeler et al. 2003) or by using the alternative semi-empirical formulations suggested by Zentar et al. (2002), Leoni et al. (2008) and Yin et al. (2011). As discussed by Karstunen and Yin (2010), the simulations are rarely sensitive to the value of ω at boundary value level.
- By using the value of $C_{\alpha e}$ (creep index) measured from conventional 1-day loading oedometer tests on intact clay samples, the values for μ^* for the ACM model can be calculated (Leoni et al. 2008). This may sound straight-forward, but the interpretation

can be difficult in the case of highly sensitive clays, when the creep index is not a soil constant (see e.g. Yin et al. 2011).

- The values for N and μ for EVP-SCLAY1 model cannot be determined directly from the experimental data. They can be calibrated by simulation of oedometer test results (see Karstunen and Yin 2010), and by their nature they are not necessarily unique. However, based on the authors' experience, the non-uniqueness is not an issue when boundary value problems such as embankments on soft clay are considered, as the predicted results with different, but yet appropriate, parameter combinations for a given clay are from practical point of view the same.
- The permeability, k_0 , is obtained from conventional 1-day loading oedometer tests on intact samples and is assumed to be the same in vertical and horizontal directions.

The selected values of parameters for Murro and Haarajoki clays used for oedometer test simulations are summarised in Tables 1-2. It is worth to emphasise that the values represent objective average values based on a whole suite of tests available at a given depth range, and hence have not been calibrated in a test by test basis.

Simulations of Element Level Tests

The element level tests that are considered in this paper are conventional 1 day oedometer tests on Murro and Haarajoki clays. Modelling 1D compression tests has been performed by simulating conventional oedometer experiments with Plaxis 2D 2010, and using EVP-SCLAY1 and/or ACM as the user defined soil model to represent the material behaviour.

Figure 3 shows the model prediction against experimental data, by plotting the predicted and measured vertical strains versus time in semi-logarithmic scale for Murro clay at a depth of 3.6 m, which represents the most compressible layer in the field. These are objective

predictions, in a way that no attempt has been made to create a best possible match, and the values of the input parameters (see Table 1) are exactly the same as used further on in the corresponding layer at the boundary value level. Therefore, the soil constants have been determined independently of the test that is being modelled. For all loading stages simulated, EVP-SCLAY1 appears to give better predictions than ACM.

In Fig. 4, similar predictions have been made for Haarajoki clay, considering two different load increments at each depth. Here the results are not as conclusive: for most stress levels and depths, EVP-SCLAY1 appears to give better prediction than ACM, but at a depth of 6.35 m and 17.22 m, ACM gives better predictions than EVP-SCLAY1 for the vertical effective stress levels of 108kPa and 330kPa, respectively. In the following, the models are compared at boundary value level. Of course, it would be possible to get a better match with ACM model by e.g. increasing POP or OCR, reference time or indeed change the values for the soil constants, in order to manipulate value of the creep exponent. That however, would be curve fitting rather than exploring objectively the model's predictive ability.

Simulations of Murro Test Embankment

In order to study model performance at boundary value level, 2D finite element simulations have been performed with 2D Version 10 of Plaxis. Murro test embankment is 2 m high and 30 m long, and the slopes have a gradient of 1:2 (see Fig. 5 for the geometry and soil layers). The groundwater table is assumed to be at the depth of 0.8 m. The embankment material is crushed rock. The construction was completed within 2 days (Karstunen et al. 2005). The embankment was modelled with a simple linear elastic-perfectly plastic Mohr-Coulomb model using the following typical values for the embankment material: $E=40,000 \text{ kN/m}^2$, $\nu=0.35$, $\phi'=40^\circ$, $\psi'=0^\circ$, $c'=2 \text{ kN/m}^2$ and $\gamma=19.6 \text{ kN/m}^3$. The values of the soil constant and state variables used are listed in Tables 3-5.

Fig. 6 plots the settlement versus time at the centreline (for the exact location of the instruments, see Karstunen and Yin 2010). EVP-SCLAY1 gives a rather good prediction, while in contrast ACM is grossly overpredicting the vertical deformations. Fig. 7 gives more insight into the reasons for this gross overprediction by ACM. The predicted settlement though by the ACM model [Fig. 7 (b)] shows non-negligible vertical deformation also outside the embankment area, indicating that significant creep strains are predicted due to the in situ stresses only. This is not realistic, of course. This is also reflected in the predicted horizontal deformations under the crest [Fig. 8] and toe [Fig. 9] of the embankment. EVP-SCLAY marginally underpredicts the horizontal movements under the crest of the embankment [Fig.8] whilst under the toe of the embankment the predictions are rather good. However, in the field, the horizontal movement develop more slowly than predicted by the rate-dependent models. Under the crest of the embankment, the location of the maximum horizontal movement is not well-predicted, whilst under the toe the depth is predicted with good accuracy.

Simulations of Haarajoki Embankment

Haarajoki test embankment is 2.9 m high and 100 m long embankment, with slope gradient of 1:2 [see Fig.10] and lateral berms for stability. Half of the embankment (50 m long section) was constructed on an area improved with prefabricated vertical drains, and the other half (Section 35840) considered for this study, was constructed on natural deposits without any ground improvement. The embankment itself was constructed in 0.5 m thick layers and each layer was applied and compacted within 2 days. The deposit consists of a 2 m thick dry crust layer overlying about 22 m of soft clay. The groundwater table is assumed to be at the ground surface. Based on the ground investigation data (FinnRA 1997) the subsoil is divided into seven sub-layers with different compressibility parameters and POP values, as

summarised in Tables 6-8. The embankment, which was made of granular fill, was modelled with a simple Mohr-Coulomb model assuming the following material parameters: $E=40,000$ kN/m², $\nu=0.35$, $\phi'=40^\circ$, $\psi'=0^\circ$, $c'=2$ kN/m² and $\gamma=21$ kN/m³.

The measured and predicted settlements at the centreline of Section 35840, as a function of time, are presented in Fig. 11. EVP-SCLAY1 is clearly underpredicting the vertical deformations whilst, yet again, ACM after a good prediction for a year or so is overpredicting the vertical deformations. Because of the presence of the vertical drains in the other section, it is likely that the field data might not be totally representative of the plane strain geometry assumed in the simulations. Namely, when looking at the vertical deformations along the longitudinal section (see Koskinen et al. 2002), the vertical deformations in Section 35840 appear to be influenced by the section with vertical drains. To confirm that, as discussed by Yildiz (2009a), the embankment would need to be modelled in 3D, albeit utilising the symmetry along the centreline.

Unlike in the case of Murro test embankment, ACM does not predict significant vertical deformations outside the embankment area [see Fig. 12]. Obviously, given POP is assumed to be > 30 kPa throughout the deposit, there is now enough overconsolidation to scale down the creep rates in the non-loaded area. However, just as in the case of Murro test embankment, ACM is also significantly overpredicting the lateral deformations. This is true for both the crest and the toe [Figs. 13(a) and 14(a)]. In contrast, EVP-SCLAY1 gives good prediction under the toe of the embankment [Fig. 15(a)].

Conclusions

The paper presents a comparison of two anisotropic rate-dependent models, ACM (Leoni et al. 2008) and EVP-SCLAY1 (Karstunen and Yin 2010). Both rate-dependent models are able to account for initial anisotropy and the evolution of anisotropy in a similar manner,

analogous to the S-CLAY1 model (Wheeler et al. 2003). However, they have differences in the mathematical formulations for calculating the creep strain rates. Simulations were done both at element level (1 day oedometer tests) and at boundary value level for Murro and Haarajoki clays. Based on the results, the EVP-SCLAY1 model that is an overstress model, is able to yield good predictions both at element level and at boundary value level in particular for the case of Murro test embankment on almost normally consolidated clay. In contrast, ACM was severely overpredicting both vertical and horizontal deformations at Murro, as unrealistic vertical deformations were triggered outside the embankment area due to the in situ stresses only. In the case of Haarajoki embankment the results were inconclusive: EVP-SCLAY1 was underpredicting deformations, whilst ACM was overpredicting them. However, the field measurements at Haarajoki are influenced by the section of the embankment that was founded on vertical drains (see Koskinen et al. 2002). Therefore, the embankment would need to be remodelled in 3D to take that effect into account.

The analyses presented in the paper ignored the effects of apparent bonding and destructuration for the sake of simplicity. For relatively sensitive clays, such as Murro clay and Haarajoki clay, this may not be appropriate and indeed, certain phenomena, such as the reduction of undrained shear strength measured under the Murro test embankment after 8 years of consolidation, reported by Koskinen and Karstunen (2006), could only be explained by rate-dependent models that account for destructuration. The same applies to phenomena such as tertiary creep and creep rupture.

Our estimations of compressibility, apparent preconsolidation stress and the tendency of a natural clay to creep are highly dependent on sample quality. The Swedish and Norwegian piston samplers that were used to extract undisturbed samples of Haarajoki and Murro clays are unlikely to result in high quality samples. This is likely to be true in particular for Murro

clay due to its high silt content. Further investigations on the effect of sample disturbance on the rate effects and deformations are needed.

Acknowledgements

The work presented was carried out as part of a Marie Curie Industry-Academia Partnerships and Pathways projects GEO-INSTALL (PIAP-GA-2009-230638) and CREEP (PIAP-GA-2011-286397). The experimental work was done at Aalto University sponsored by Academy of Finland (Grant 128459).

Appendix A. Model Formulations

In the following, compression has been assumed as positive, following the geotechnical tradition.

Formulation of EVP-SCLAY1 Model

The constitutive model EVP-SCLAY1 (Karstunen and Yin 2010) is based on the overstress theory of Perzyna (Perzyna 1963) and the elasto-plastic model SCLAY1 (Wheeler et al. 2003). According to Perzyna's overstress theory, the total strain rate is additively composed of the elastic strain rates and viscoplastic strain rates

$$\dot{\epsilon}_{ij} = \dot{\epsilon}_{ij}^e + \dot{\epsilon}_{ij}^{vp} \quad (a1)$$

where $\dot{\epsilon}$ denotes the (i,j) component of the total strain rate tensor, and the superscripts e and vp stand, respectively, for the elastic and the viscoplastic components. The elastic behaviour

in the proposed model is assumed to be isotropic in a similar way to the Modified Cam Clay model (Roscoe and Burland 1968).

An elliptical surface, relating to the current state of preconsolidation, is adopted as the static yield surface

$$f = \frac{3}{2} [\sigma'_d - p' \alpha_d] : [\sigma'_d - p' \alpha_d] - \left(M^2 - \frac{3}{2} [\alpha_d] : [\alpha_d] \right) (p'_m - p') p' = 0 \quad (\text{a2})$$

where σ'_d is the deviatoric stress tensor ($\sigma'_d = \sigma'_{ij} - p' \delta_{ij}$), with Kronecker's delta ($\delta_{ij} = 1$ for $i = j$ and $\delta_{ij} = 0$ for $i \neq j$); p' is the mean effective stress; α_d is the deviatoric fabric tensor, a dimensionless vector with the same form as the deviatoric stress vector (Wheeler et al. 2003); M is the slope of the critical state line. For the special case of a cross-anisotropic sample in triaxial stress space, the scalar parameter $\alpha = \sqrt{3/2(\alpha_d : \alpha_d)}$ defines the inclination of the ellipse of the yield curve in the $p' - q$ plane as illustrated in Fig. 1(a). The dynamic loading surface has an identical shape, but a different size $p'_m{}^d$ [see Fig. 1(a)] compared to the static yield surface. To represent the dynamic loading surface Eq. (a2) can be rewritten as

$$f_d = \frac{(3/2) [\sigma'_d - p' \alpha_d] : [\sigma'_d - p' \alpha_d]}{(M^2 - (3/2) [\alpha_d] : [\alpha_d]) p'} + p' - p'_m{}^d = 0 \quad (\text{a3})$$

The viscoplastic strain rate in Eq. (a1) is assumed to obey an associated flow rule with respect to the dynamic loading surface. The incremental viscoplastic strains in the EVP-SCLAY1 model (Karstunen and Yin 2010) can be calculated as

$$\dot{\varepsilon}_{ij}^{vp} = \mu \left\langle \exp \left[N \cdot \left(\frac{p'_m{}^d}{p'_m} - 1 \right) \right] - 1 \right\rangle \frac{\partial f_d}{\partial \sigma'_{ij}} \quad (\text{a4})$$

where μ is referred to as the fluidity parameter; $\langle \rangle$ are McCauley brackets; N is the strain-rate coefficient relating to the strain-rate effect on shear strength and preconsolidation

pressure. N and μ are therefore the key parameters controlling the viscoplastic strain-rate. Symbols p_m^d and p_m^s represent the size of dynamic loading surface and the static yield surface, respectively [see Fig. 1(a)] and f_d is the viscoplastic potential function, represented by the dynamic loading surface.

The expansion of the static yield surface, which represents the kinematic hardening of the material, is assumed to be due to the viscoplastic volumetric strain rate $\dot{\epsilon}_v^{vp}$, similarly to the critical state models

$$\dot{p}_m^s = p_m^s \left(\frac{1+e}{\lambda - \kappa} \right) \dot{\epsilon}_v^{vp} \quad (\text{a5})$$

where λ is the slope of the normal compression curve in the $e - \ln \sigma'_v$ plane, κ is the slope of the swelling line and e is the void ratio.

The rotational hardening law that controls the development or erasure of anisotropy caused by viscoplastic strains, is defined based on the formulation proposed by Wheeler et al. (2003). Both volumetric and deviatoric viscoplastic strains influence the rotation of the yield surface

$$\dot{\alpha}_d = \omega \left(\left[\frac{3\eta_d}{4} - \alpha_d \right] \langle \dot{\epsilon}_v^{vp} \rangle + \omega_d \left[\frac{\eta_d}{3} - \alpha_d \right] \dot{\epsilon}_d^{vp} \right) \quad (\text{a6})$$

where dots again refer to rates. In the above η_d is the tensorial equivalent of the stress ratio defined as $\eta_d = \sigma_d / p'$, ω and ω_d are additional soil constants that control, respectively, the absolute rate of the rotation of the yield and loading surfaces toward their current target values, and the relative effectiveness of viscoplastic volumetric and deviatoric strains in rotating the yield and loading surfaces and $\dot{\epsilon}_d^{vp}$ is the viscoplastic deviatoric strain rate.

Formulation of ACM Model

In the ACM model the total strain rate is additively composed of the elastic strain rates and (irrecoverable) creep strain rates, using superscript c to denote creep

$$\dot{\epsilon}_{ij} = \dot{\epsilon}_{ij}^e + \dot{\epsilon}_{ij}^c \quad (\text{a7})$$

In the ACM model (Leoni et al. 2008) a so-called equivalent mean stress p'_{eq} is defined as

$$p'_{eq} = p' + \frac{(3/2) [\sigma'_d - p' \alpha_d] : [\sigma'_d - p' \alpha_d]}{(M^2 - (3/2) [\alpha_d] : [\alpha_d]) p'} \quad (\text{a8})$$

which represents the size of the current stress surface (CSS). This is analogous to the static yield surface in Eq. (a2). CSS cannot be called a yield surface in a classical sense, as with the ACM model it is possible to have irrecoverable creep strains everywhere in the stress space. However, within the normal consolidation surface (NCS) of the ACM model, defined with Eq. (a8) by substituting p'_{eq} with p'_p [see Fig. 1(b)] the creep strains are albeit possible but they are small indeed. In the ACM model the preconsolidation pressure p'_p evolves with the volumetric creep rate according to the hardening law, which is analogous to Eq. (a5), but expressed in terms of modified compression and swelling indexes λ^* and κ^* , where $\lambda^* = \lambda / (1 + e_0)$ and $\kappa^* = \kappa / (1 + e_0)$ are the modified compression and swelling indexes respectively. This can be expressed in integrated format as

$$p'_p = p'_{p0} \exp\left(\frac{\dot{\epsilon}_v^c}{\lambda^* - \kappa^*}\right) \quad (\text{a9})$$

When $p'_{eq} = p'_p$, the current stress state lies on the normal consolidation surface [Fig. (1b)], and the soil state is normally consolidated, and as a consequence large creep strains occur. The ratio p'_p / p'_{eq} (referred to as OCR^*), gives a measurement of the distance between the current stress surface and the normal consolidation surface, being a generalisation of OCR. In

the ACM model the NC surface is treated as the contour of constant volumetric creep, so the incremental volumetric creep strains are calculated as

$$\dot{\varepsilon}_v^c = \frac{\mu^*}{\tau} \left(\frac{p'_{eq}}{p'_p} \right)^{\frac{\lambda^* - \kappa^*}{\mu^*}} \quad (\text{a10})$$

where is μ^* is the modified creep index (slope of $\varepsilon_v - \ln t$ plot) and τ is a reference time. As discussed by Leoni et al. (2008), the concept of a reference time makes this type of model very attractive, as it enables to scale the input for over-consolidation ratio dependant on the strain-rate in the test. The deviatoric component of the creep strain rate vector can be obtained from the flow rule, which is assumed to be associated. The rotational hardening law in the ACM model is similar to that of EVP-SCLAY1 model

$$\dot{\alpha}_d = \omega \left(\left[\frac{3\eta_d}{4} - \alpha_d \right] \langle \dot{\varepsilon}_v^c \rangle + \omega_d \left[\frac{\eta_d}{3} - \alpha_d \right] \dot{\varepsilon}_d^c \right) \quad (\text{a11})$$

References

- Finnish National Road Administration (FinnRA). (1997). "Competition to calculate settlements at the Haarajoki test embankment." Competition programme, competition materials, FinnRA, Finland.
- Hinchberger, S. D., and Qu, G. (2009). "Viscoplastic constitutive approach for rate-sensitive structured clays." *Can. Geotech. J.*, 46(6), 609-626.
- Karstunen, M., and Koskinen, M. (2004). "Anisotropy and destructuration of Murro clay." *Proc., Advances in Geotechn. Eng. Skempton Conf.*, London, UK, 1, 476-487.

- Karstunen, M., and Koskinen, M. (2008). "Plastic anisotropy of soft reconstituted clays." *Can. Geotech. J.*, 45(3), 314-328.
- Karstunen, M., Krenn, H., Wheeler, S. J., Koskinen, M., and Zentar, R. (2005). "The effect of anisotropy and destructuration on the behaviour of Murro test embankment." *Int. J. Geomech.*, 5(2), 87-97.
- Karstunen, M., and Yin, Z. -Y. (2010). "Modelling time-dependent behaviour of Murro test embankment." *Géotechnique*, 60(10), 735-749.
- Koskinen M., and Karstunen M. (2006). "Numerical modelling of Murro test embankment with S-CLAY1S." *Proc. 6th Eur. Conf. Num. Methods Geotech. Engineering*, Graz, Austria, 11-19.
- Koskinen, M., Karstunen, M., and Wheeler, S. J. (2002). "Modelling destructuration and anisotropy of a natural soft clay." *Proc., 5th European Conf. on Numerical Methods in Geotech. Engineering (NUMGE)*, Paris, Presses de l'ENPC, France, 11-20.
- Leoni, M., Karstunen, M., and Vermeer, P. A. (2008). "Anisotropic creep model for soft soils." *Géotechnique*, 58(3), 215–226.
- Perzyna, P. (1963). "The constitutive equations for work-hardening and rate sensitive plastic materials." *Proc. Vibration Problems Warsaw*, 3, 281-290.

- Qu, G., Hinchberger, S. D., and Lo, K. Y. (2010). "Evaluation of the viscous behaviour of clay using generalised overstress viscoplastic theory." *Géotechnique*, 60(10) 777-789.
- Roscoe, K. H., and Burland, J. B. (1968). "On the generalized stress-strain behaviour of 'wet' clay." I, Cambridge University Press, Cambridge, U.K., 553-609.
- Wheeler, S. J., Näätänen, A., Karstunen, M., and Lojander, M. (2003). "An anisotropic elasto-plastic model for soft clays." *Can. Geotech. J.*, 40(2), 403-418.
- Yildiz, A. (2009a). "Numerical modeling of vertical drains with advanced constitutive models." *Comput. Geotech.*, 36(6), 1072-1083.
- Yildiz, A., Karstunen, M., and Krenn, H. (2009b). "Effect of anisotropy and destructuration on behavior of Haarajoki test embankment." *Int. J. Geomech.*, 9(4), 153-168.
- Yin, Z. -Y., Chang, C. S., Karstunen, M., and Hicher, P. Y. (2010). "An anisotropic elastic-viscoplastic model for soft clays." *Int. J. Solids Struct.*, 47(5), 665-677.
- Yin, Z. -Y., Karstunen, M., Chang, C. S., Koskinen, M., and Lojander, M. (2011). "Modeling time-dependent behavior of soft sensitive clay." *J. Geotech. Geoenviron. Eng.*, 137(11), 1103-1113.
- Zentar, R., Karstunen, M., and Wheeler, S. J. (2002). "Influence of anisotropy and destructuration on undrained shearing of natural clays." *Proc., 5th European Conf. on*

Numerical Methods in Geotech. Engineering (NUMGE), Paris, Presses de l'ENPC, France,
21–26.

Zhou, C., Yin, J.-H., Zhu, J.-G., and Cheng, C.-M. (2006). “Elastic anisotropic viscoplastic modeling of the strain-rate dependent stress–strain behaviour of K_0 -consolidated natural marine clays in triaxial shear test.” *Int. J. Geomech.*, 5(3), 218-232.

Accepted Manuscript
Not Copyedited

Figure captions

Fig. 1. a) Yield surfaces of the EVP-SCLAY1 model; b) Normal consolidation surface and current stress surface of ACM model

Fig. 2. Yield surfaces of Murro clay at a depth of 4m and 7m. Data after Karstunen and Yin (2010)

Fig. 3. Conventional oedometer test predictions of Murro clay

Fig. 4. Conventional oedometer test predictions of Haarajoki clay

Fig. 5. Geometry of Murro test embankment

Fig. 6. Time-settlement predictions for Murro test embankment. Field data from Karstunen and Yin (2010)

Fig. 7. Surface settlements of Murro test embankment a) EVP-SCLAY1; b) ACM. Field data from Karstunen and Yin (2010)

Fig. 8. Lateral displacement predictions under the crest of Murro test embankment a) EVP-SCLAY1; b) ACM. Field data from Karstunen and Yin (2010)

Fig. 9. Lateral displacement predictions under the toe of Murro test embankment a) EVP-SCLAY1; b) ACM. Field data from Karstunen and Yin (2010)

Fig. 10. Geometry of Haarajoki embankment

Fig. 11. Time-settlement predictions of Haarajoki embankment (Section 35840). Field data from Yildiz et al. (2009b)

Fig. 12. Surface settlements of Haarajoki embankment a) EVP-SCLAY1; b) ACM. Field data from Yildiz et al. (2009b)

Fig. 13. Comparison of lateral displacement predictions at the crest of Haarajoki embankment. Field data from Yildiz et al. (2009b)

Fig. 14. Comparison of lateral displacement predictions at the toe of Haarajoki embankment. Field data from Yildiz et al. (2009b)

Table 1. Parameter values for Murro clay at a depth of 3.6 m

λ	κ	e_0	POP (kPa)	v'	M	α_{k0}	ω	ω_d	EVP-SCLAY1		ACM	
									N	μ (day ⁻¹)	μ^*	τ (day)
0.5	0.041	2.44	1.0	0.3	1.65	0.66	20	1.02	20	8.64E-5	1.92E-3	1

Accepted Manuscript
Not Copyedited

Table 2. Parameter values for Haarajoki clay at a depth of 6.4 m

λ	κ	e_0	POP (kPa)	v'	M	α_{K0}	ω	ω_d	EVP-SCLAY1		ACM	
									N	μ (day ⁻¹)	μ^*	τ (day)
0.96	0.03	2.6	32.0	0.2	1.43	0.55	49	0.97	18	6E-6	3.47E-3	1

Accepted Manuscript
Not Copyedited

Table 3. The initial values for the state parameters for Murro test embankment

Layer	Depth (m)	POP (kPa)	e_0	α_{K0}
1-1	0.0 – 0.8	20	1.4	0.63
1-2	0.8 – 1.6	10	1.4	0.63
2	1.6 – 3.0	1	1.8	0.63
3	3.0 – 6.7	1	2.4	0.63
4	6.7 – 10.0	1	2.1	0.63
5	10.0 -15.0	1	1.8	0.63
6	15.0 – 23.0	1	1.5	0.63

Accepted Manuscript
Not Copyedited

Table 4. The values for the conventional soil parameters and additional soil constants for Murro test embankment

Layer	γ (kN/m ³)	v'	M	k_x (m/day)	k_y (m/day)	ω	ω_d	EVP-SCLAY1		ACM	
								λ	κ	λ^*	κ^*
1-1	15.8	0.35	1.6	2.13E-4	1.64E-4	45	1.02	0.16	0.010	0.0667	4.20E-3
1-2	15.8	0.35	1.6	2.13E-4	1.64E-4	45	1.02	0.16	0.010	0.0667	4.20E-3
2	15.5	0.35	1.6	2.13E-4	1.64E-4	25	1.02	0.50	0.030	0.1786	1.07E-2
3	14.9	0.10	1.6	1.78E-4	1.34E-4	20	1.02	0.50	0.036	0.1471	1.06E-2
4	15.1	0.15	1.6	1.10E-4	9.07E-5	25	1.02	0.36	0.030	0.1161	9.70E-3
5	15.5	0.15	1.6	6.85E-5	5.48E-5	25	1.02	0.32	0.034	0.1143	1.21E-2
6	15.9	0.15	1.6	1.04E-4	8.22E-5	30	1.02	0.14	0.004	0.056	1.60E-3

Accepted Manuscript
 Not Copyedited

Table 5. The values of viscosity parameters for Murro test embankment

Layer	EVP-SCLAY1		ACM	
	N	μ (day ⁻¹)	μ^*	τ (day)
1-1	25	8.64E-8	8.69E-4	1
1-2	25	8.64E-8	8.69E-4	1
2	11	2.59E-7	2.33E-3	1
3	20	8.64E-5	1.92E-3	1
4	9	6.91E-4	1.51E-3	1
5	25	4.32E-5	1.49E-3	1
6	12	8.64E-4	7.30E-4	1

Accepted Manuscript
Not Copyedited

Table 6. The initial values for the state parameters for Haarajoki embankment

Layer	Depth (m)	POP (kPa)	e_0	α_{K0}
1	0. – 2.	110	1.25	0.63
2	2. – 6.	32	2.9	0.44
3	6. – 7.	32	2.6	0.55
4	7. – 12.	32	2.35	0.44
5	12. – 15.	32	2.2	0.46
6	15. -18.	32	2.0	0.61
7	18. – 22.	32	1.25	0.61

Accepted Manuscript
Not Copyedited

Table 7. The values for the conventional soil parameters and additional soil constants for Haarajoki embankment

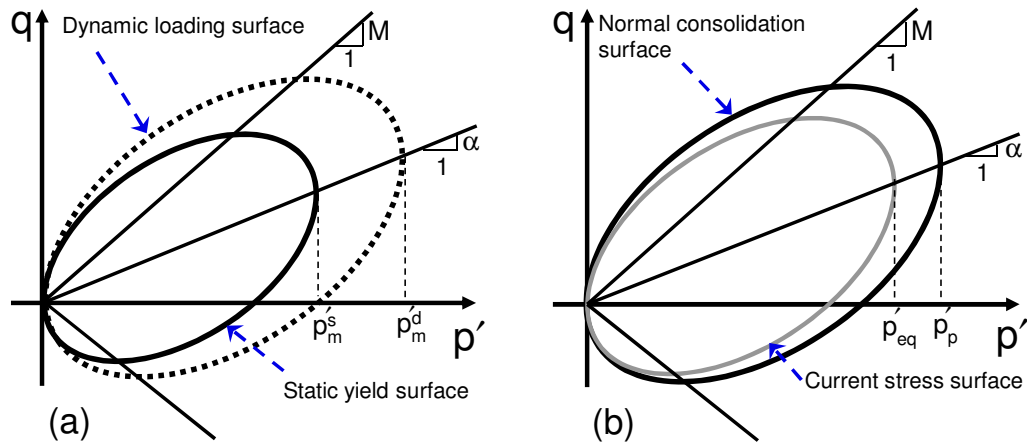
Layer	γ (kN/m ³)	v'	M	k_x (m/day)	k_y (m/day)	ω	ω_d	EVP-SCLAY1		ACM	
								λ	κ	λ^*	κ^*
1	17.5	0.2	1.6	3.46E-4	1.73E-4	37	1.02	0.2	0.010	0.089	8.89E-3
2	14.3	0.2	1.15	1.04E-4	5.18E-5	33	0.70	1.33	0.010	0.341	1.54E-2
3	14.3	0.2	1.43	8.64E-5	4.32E-5	49	0.97	0.96	0.030	0.267	1.17E-2
4	15.1	0.2	1.15	8.64E-5	4.32E-5	44	0.70	0.96	0.036	0.287	1.25E-2
5	15.1	0.2	1.20	8.64E-5	4.32E-5	35	0.76	1.06	0.030	0.331	8.75E-3
6	15.7	0.2	1.55	8.64E-5	4.32E-5	36	1.01	0.45	0.034	0.15	1.23E-2
7	17.5	0.2	1.55	3.46E-4	1.73E-4	37	1.01	0.10	0.004	0.044	8.89E-3

Accepted Manuscript
 Not Copyedited

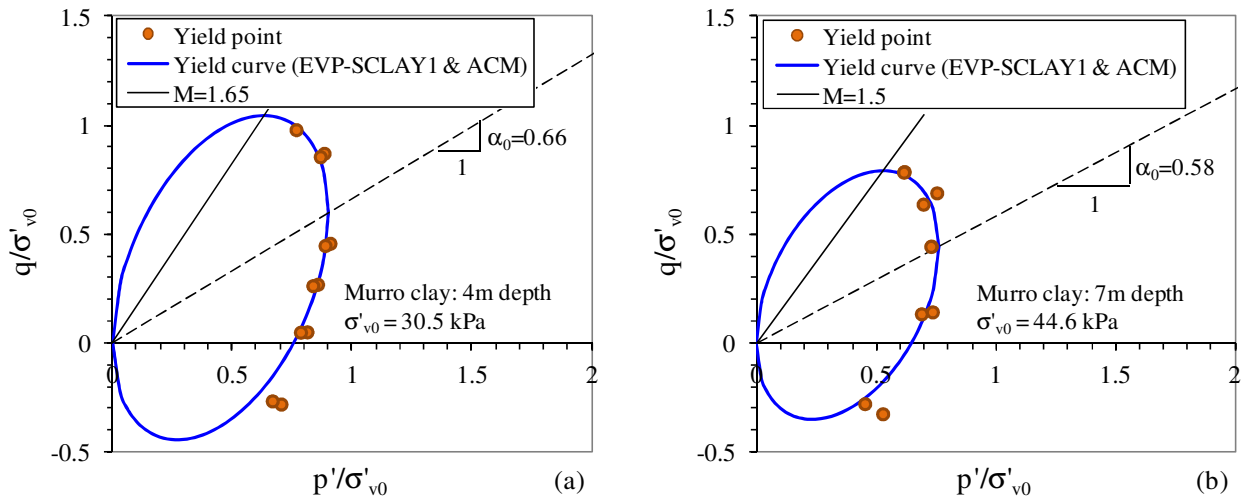
Table 8. The values for viscosity parameters for Haarajoki embankment

Layer	EVP-SCLAY1		ACM	
	N	μ (day ⁻¹)	μ^*	τ (day)
1	20	8E-4	1.16E-3	1
2	18	8E-4	4.44E-3	1
3	18	6E-6	3.47E-3	1
4	18	6E-6	3.73E-3	1
5	30	8E-5	4.32E-3	1
6	60	5E-4	1.95E-3	1
7	60	5E-4	5.79E-4	1

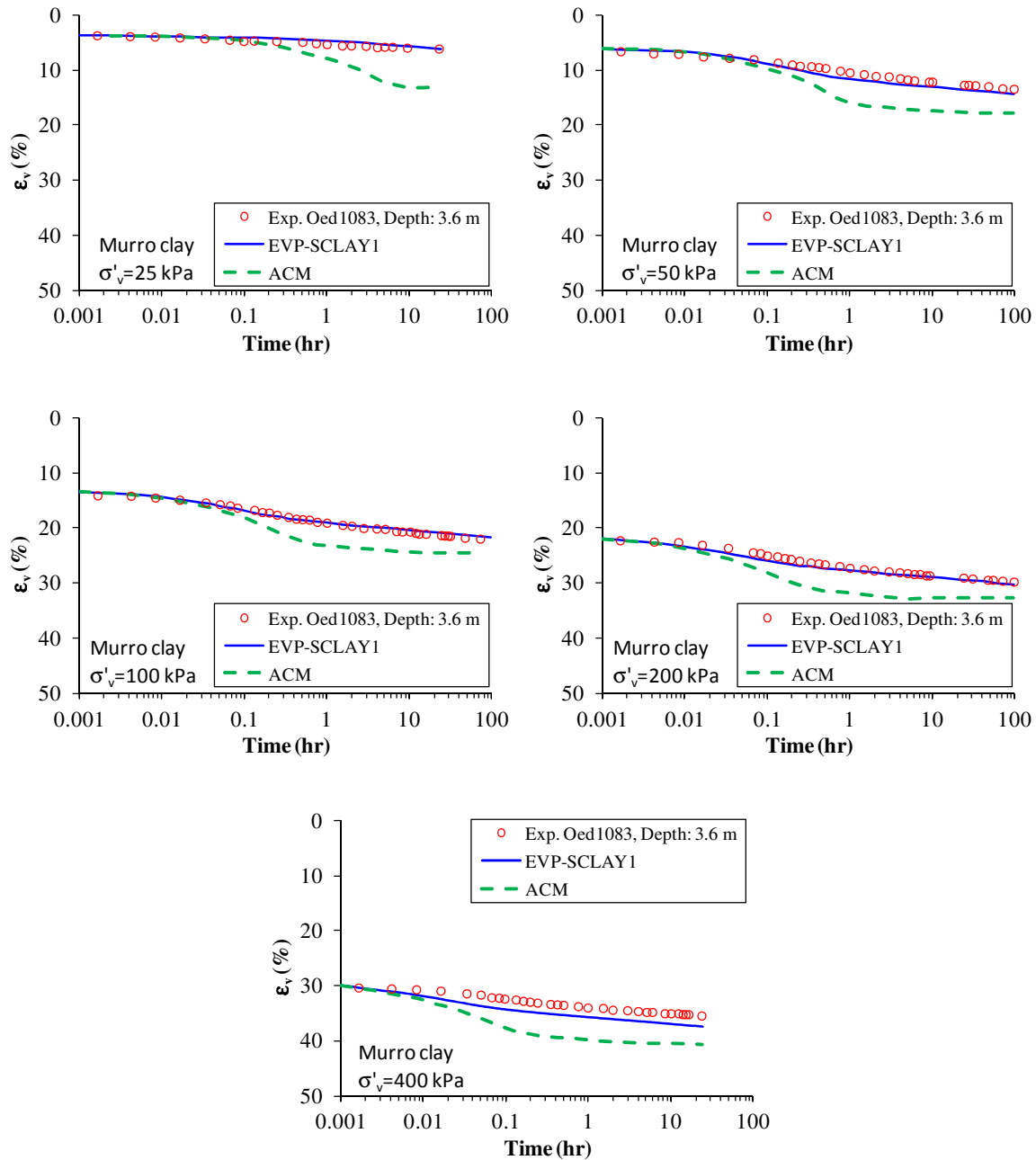
Accepted Manuscript
Not Copyedited



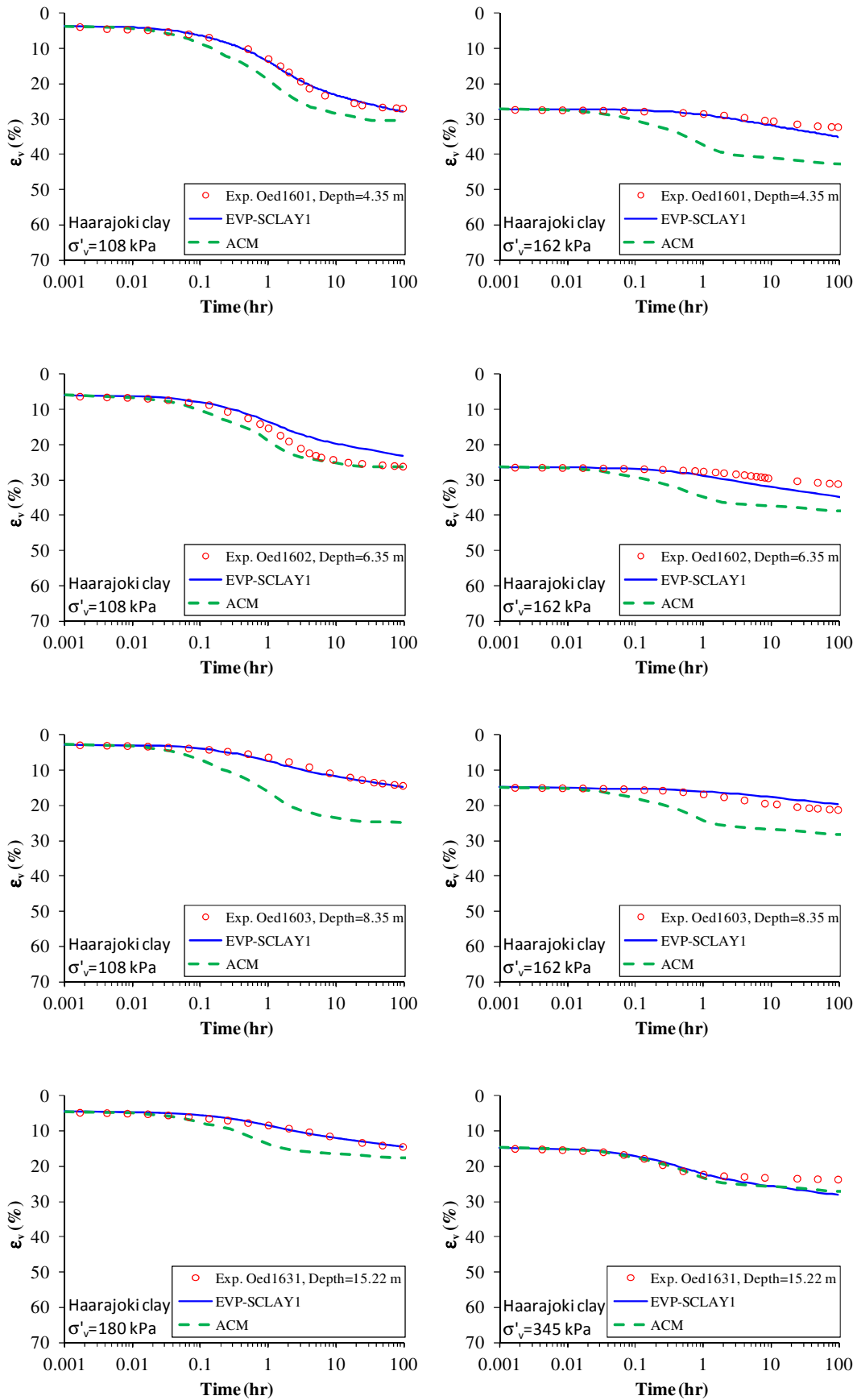
Accepted Manuscript
Not Copyedited



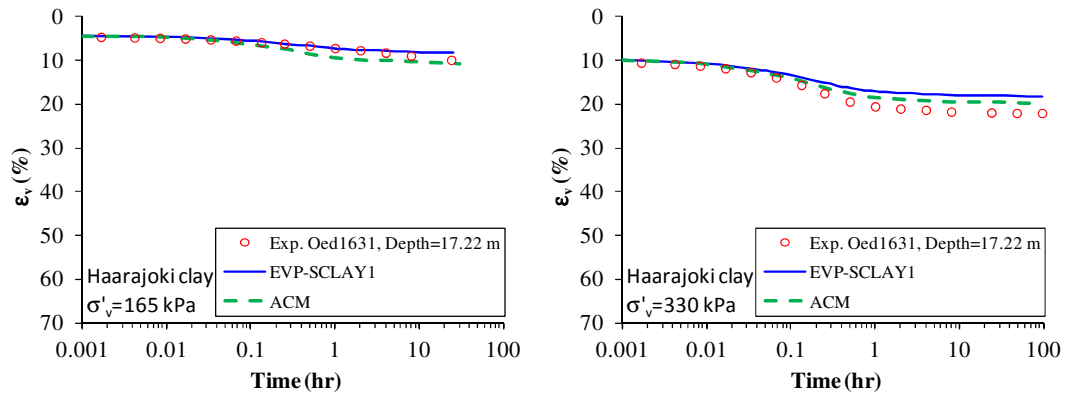
Accepted Manuscript
Not Copyedited



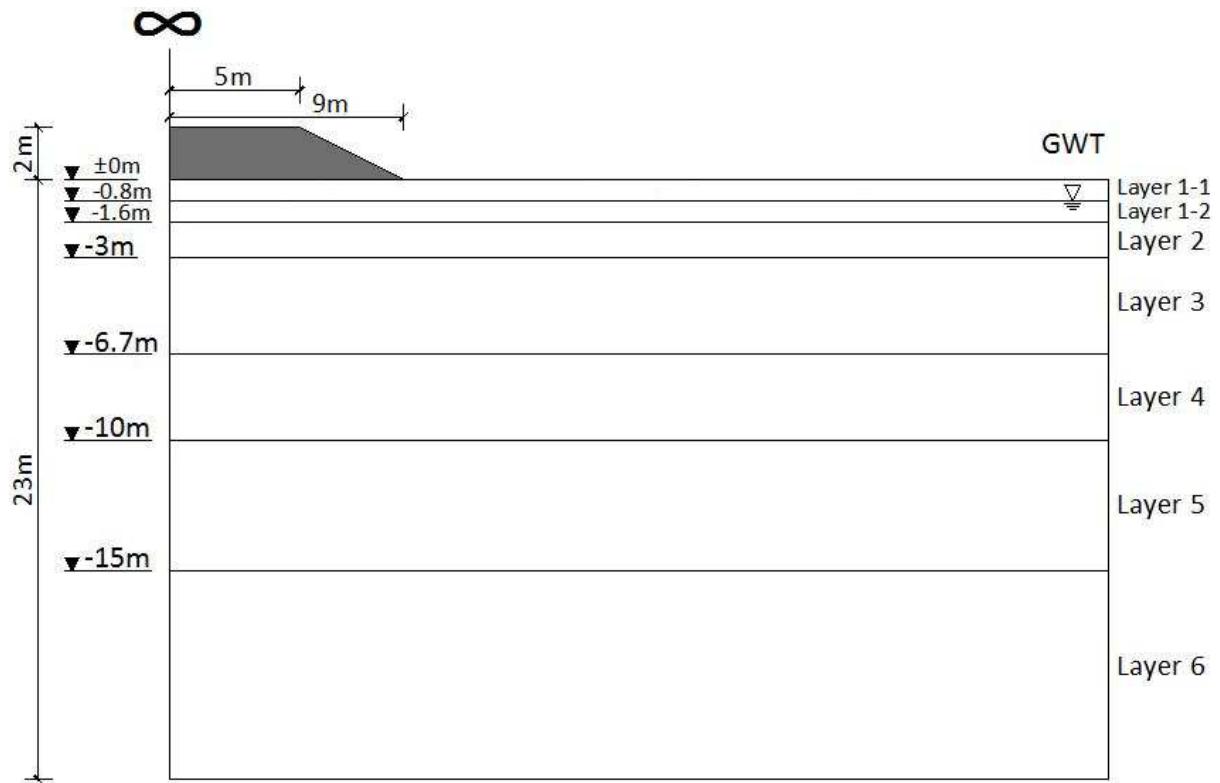
Accepted Manuscript
Not Copyedited



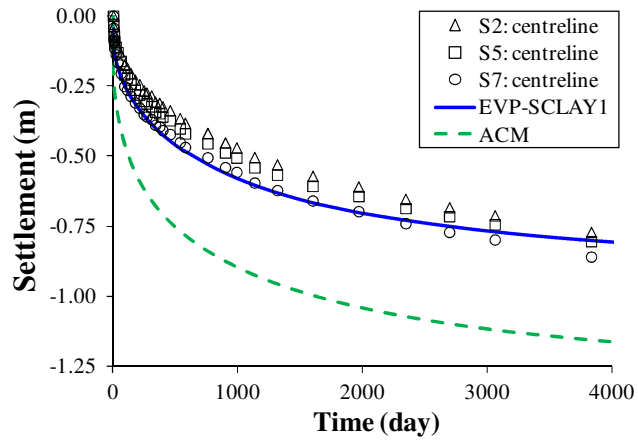
Accepted Manuscript
Not Copied



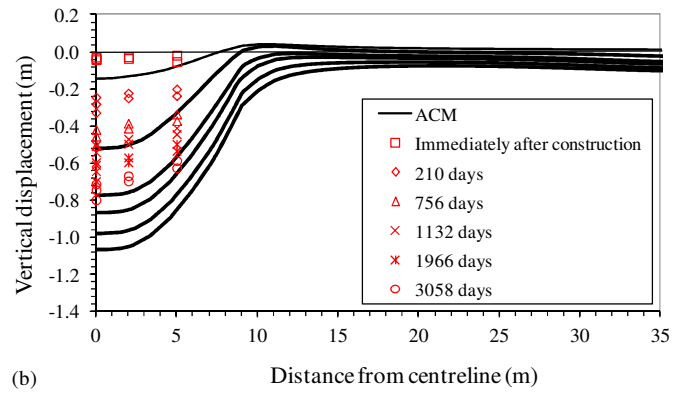
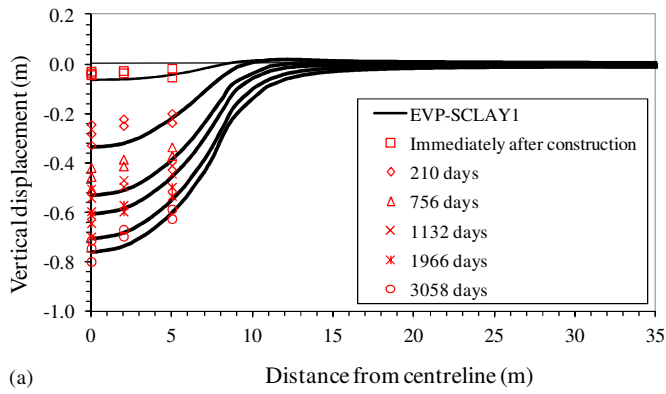
Accepted Manuscript
Not Copyedited



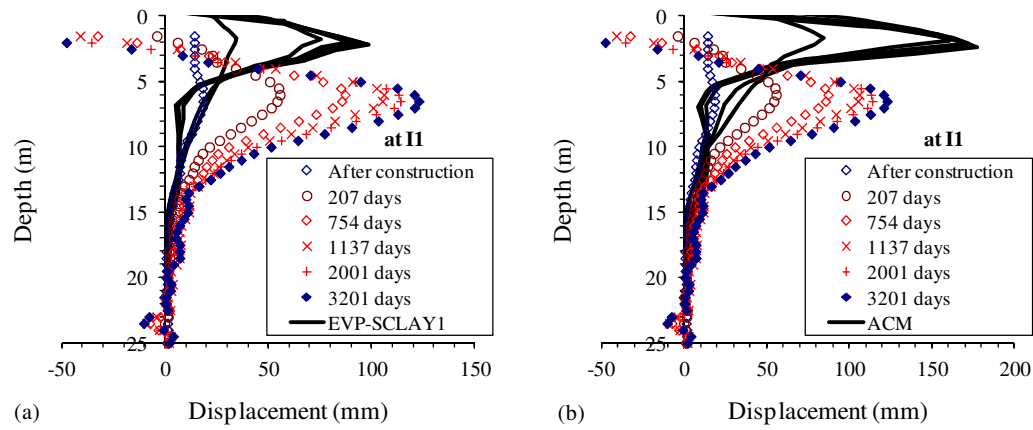
Accepted Manuscript
Not Copyedited



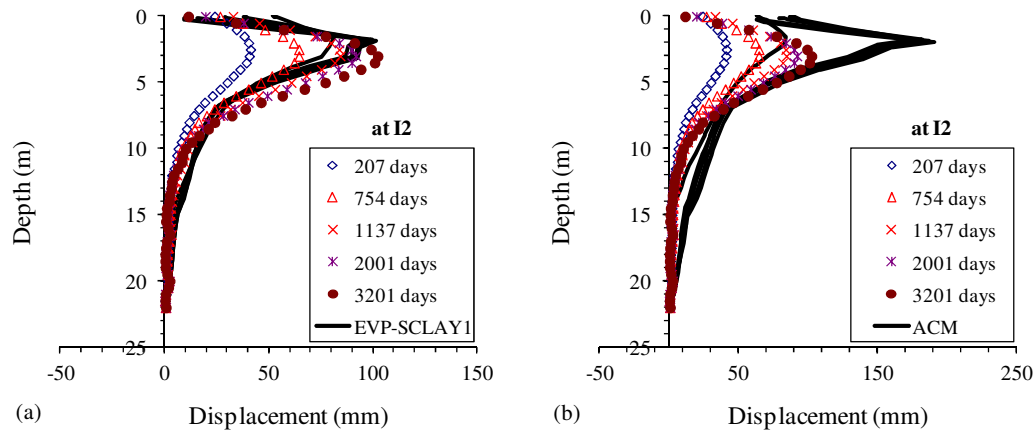
Accepted Manuscript
Not Copyedited



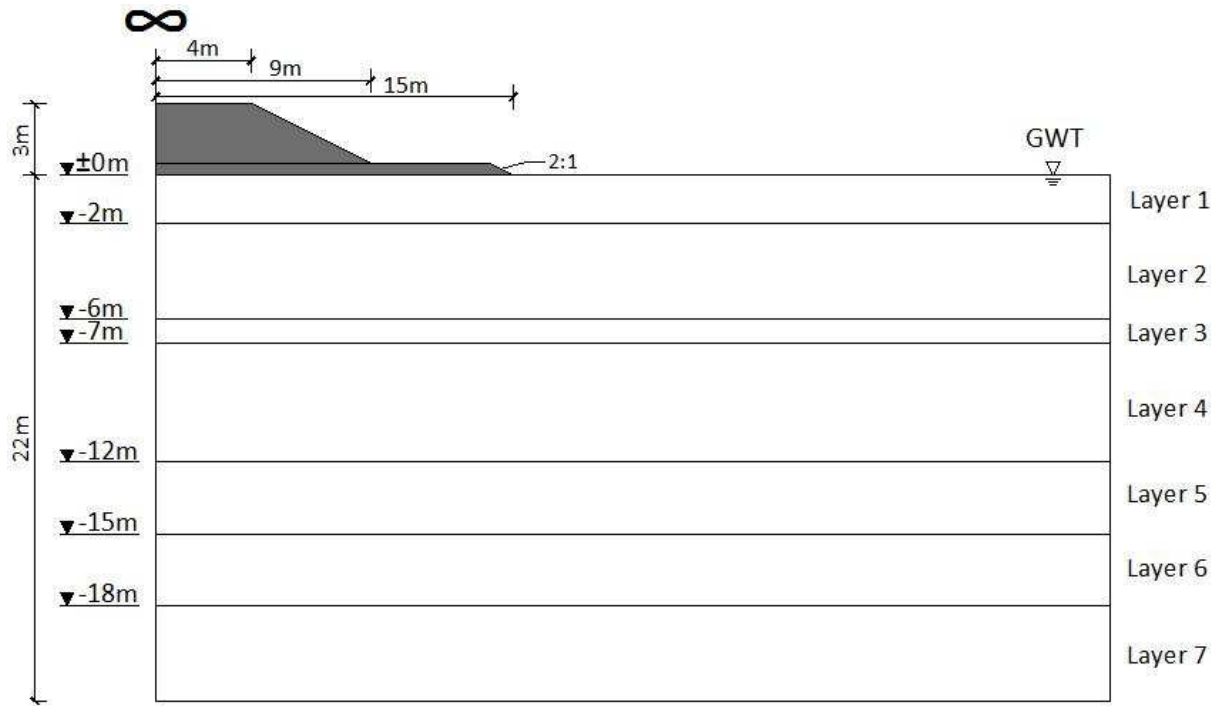
Accepted Manuscript
Not Copyedited



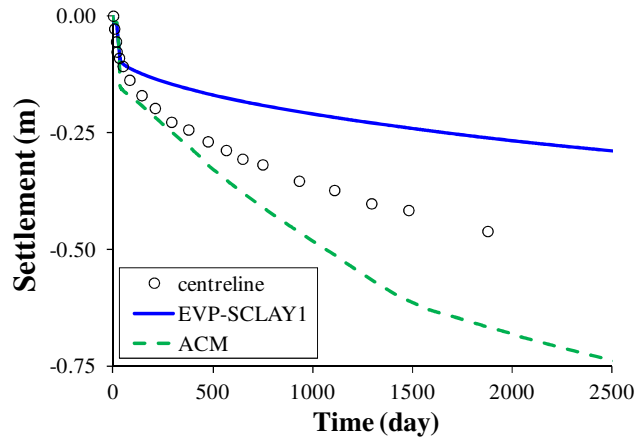
Accepted Manuscript
Not Copyedited



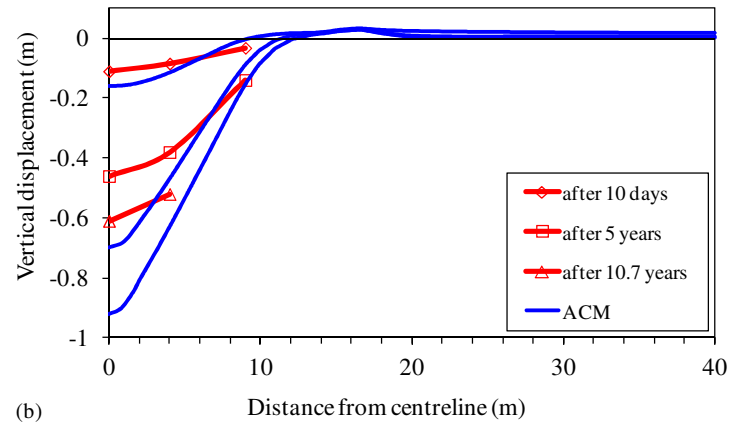
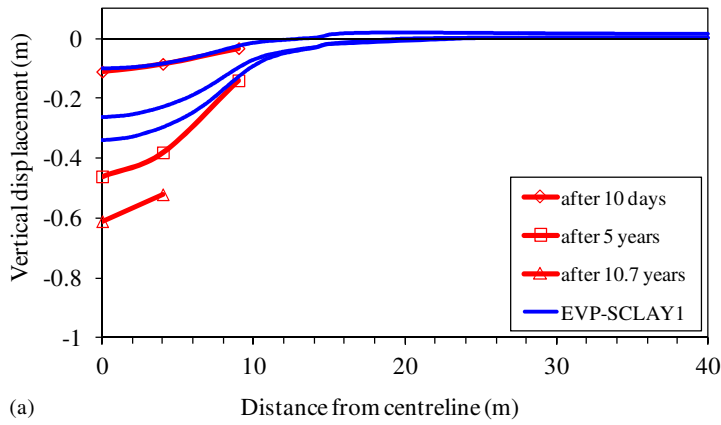
Accepted Manuscript
Not Copyedited



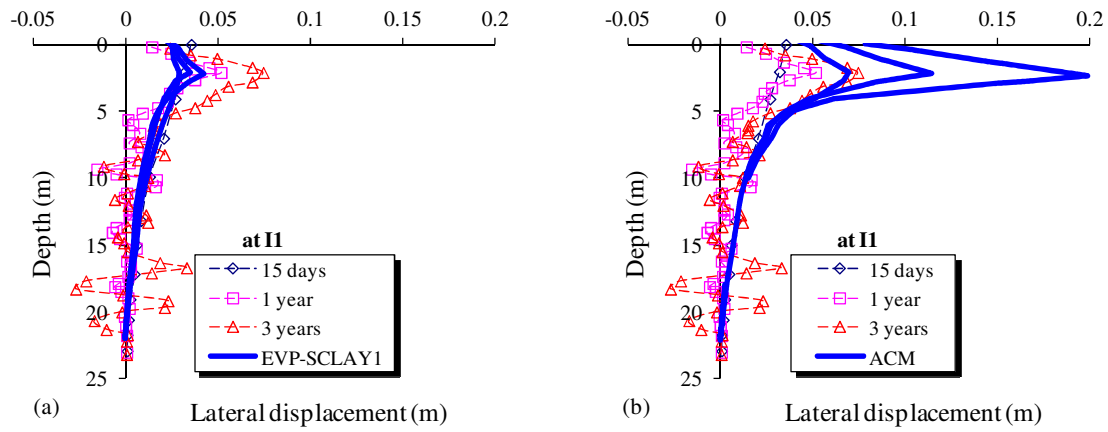
Accepted Manuscript
Not Copyedited



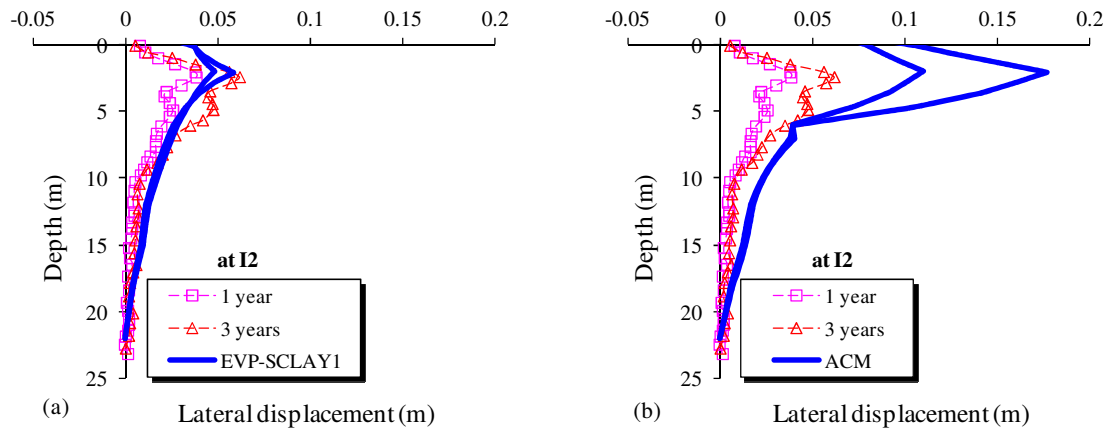
Accepted Manuscript
Not Copyedited



Accepted Manuscript
Not Copyedited



Accepted Manuscript
Not Copyedited



Accepted Manuscript
Not Copyedited